Proceedings of the ASME-JSME-KSME 2011 Joint Fluids Engineering Conference
AJK-Fluids2011
July 24-29, 2011, Hamamatsu, Shizuoka, JAPAN

AJK2011-21015

CHARACTERISTICS OF THE SCALAR FIELD IN A TURBULENT LIQUID JET AND A FUNDAMENTAL STUDY ON THE MICRO SCALE CONCENTRATION MEASUREMENTS BY THE OPTICAL FIBER LIF METHOD

Tatsuya Kawaguchi
Nagoya Univercity
Nagoya, Aichi, Japan

Yasuhiko Sakai
Nagoya Univercity
Nagoya, Aichi, Japan

Kouji Nagata
Nagoya Univercity
Nagoya, Aichi, Japan

Osamu Terashima
Nagoya Univercity
Nagoya, Aichi, Japan

Shoichi Takaku
Nagoya Univercity
Nagoya, Aichi, Japan

ABSTRACT

In this study, the characteristics of the scalar field in an axisymmetric turbulent water jet are investigated experimentally. In the experiments, the axial velocity, the concentration of the dye solution and the temperature of the fluid are measured by the hot-film probe, the fiber sensor and the cold-firm probe, respectively. In particular, the difference of statistics between scalars (concentration and temperature) with the different molecular diffusion coefficients is discussed. The Schmidt number of the diffusing matter is 3,800, and the Prandtl number of temperature is 7. As regarding the mean values, the r.m.s values and distribution of PDF, we cannot find any difference between the concentration field and temperature field. However, in the spectrum, it is found that the temperature spectrum shows the -5/3 law almost in the same range as the velocity spectrum, on the other hand, the concentration spectrum shows the -5/3 law in the wider range than the velocity spectrum. This means that the shape of spectrum depends on the diffusion coefficient.

In order to make the higher resolution measurement of concentration, a new optical probe based on the LIF method is designed. This probe consists of the two optical fibers, the tip of which is processed like the shape of a lens. By the effect of lens, the laser beam can be focused on the narrower area in comparison with the past LIF measurements. In the present design, the width of focus of laser beam is set to 0.6 micrometers, and the focal length is set to 7.3mm. It is shown that this probe has the resolution less than the Batchelor scale at $x/d \geq 30$ in the condition of present jet diffusion field (d=4mm, Re=20,000). Further, a new system to adjust the position of the optic fiber probe exquisitely is developed.

INTRODUCTION

There are many practical problems in the industrial and natural flow fields that the diffusing matter are mixed. In this study, we pay a special attention to the diffusion fields of scalars (concentration and temperature) in the turbulent liquid jet. In the liquid phase, it is usually known that the Schmidt number of the diffusing matter (or the Prandtl number in case of temperature) is larger than 1, so that the scalar fields have been crucially influenced by the velocity field. In this case, it is useful to investigate the relations between the velocity and scalar statistics to understand the mixing process of the scalar in the turbulent liquid flows.

With regard to the measurements of high Schmidt number matter, the concentrations of the fluorescent dye or the kalium chloride have been often measured by Laser-Induced Fluorescence (LIF) method or the electrode method. However seeing the past reports, in case of the flows with the mean shear, there are still large scattering of the data for the scalar statistics, and so the reliable turbulent statistics are keenly required.

On the other hand, the similarity theory of turbulent scalar field shows that for the scalar field of high Schmidt number and high Reynolds number, there exist the statistical universal ranges called the “viscous convective subrange” and the “viscous diffusive subrange” in the space smaller than the Kolmogorov scale (which is the smallest velocity fluctuation

scale). These viscous convective and diffusive subranges correspond to the final stage of the scalar cascade process, but its statistical characteristics are still not clarified well.

From the above background, in this study, the characteristics of the scalar field in a turbulent liquid jet which is one of the typical turbulent flow are investigated. In particular, the Schumidt number (Prandtl number) dependence for the statistics of the scalar fields (concentration and temperature) is discussed. Further, for higher resolution measurement in concentration field, a fundamental study on the micro scale concentration measurements by the optical fiber LIF method is performed.

NOMENCLATURE

x	axial coordinate (see Fig.1)
r	radial coordinate (see Fig.1)
d	nozzle diameter
$\langle U \rangle$	mean axial velocity
u	fluctuating axial velocity
u'	r.m.s. value of fluctuating axial velocity
b_U	half width of mean axial velocity
t_{uI}	integral time scale of axial velocity
$E_u(f)$	power spectrum of fluctuating axial velocity
$\langle C \rangle$	mean concentration
c	fluctuating concentration
c'	r.m.s. value of fluctuating concentration
b_c	half width of mean concentration
t_{cI}	integral time scale of concentration
$E_c(f)$	power spectrum of fluctuating concentration
$\langle \Theta \rangle$	mean temperature
θ	fluctuating temperature
θ'	r.m.s. value of fluctuating temperature
b_Θ	half width of mean temperature
$t_{\theta I}$	integral time scale of temperature
$E_\Theta(f)$	power spectrum of fluctuating temperature
Re	Reynolds number
Sc	Schmidt number
Pr	Prandtl number

Subscripts

$()_0$	related to the nozzle exit
$()_c$	related to the axis

EXPERIMENTAL APPARATUS AND CONDITION

Figure 1 shows the schematic of the experimental apparatus. The size of the open tank is 350mm (height) × 300mm (width) × 1,200mm (length). The water level is adjusted to 300mm. The nozzle of the exit diameter d=4.0mm is set horizontal at the center of the cross section of the tank. The coordinate system is the cylindrical one whose origin is at the center of nozzle exit, and x and r are the axial direction and radial direction, respectively.

The I-type hot-film sensor (TSI 1210-20W) and the constant temperature hot-wire velocimeter (HAYAKAWA HC-30) are used for instantaneous velocity measurement. The length and diameter of the sensing element of hot-film probe are 1mm and 51μm, respectively.

Fiber optic probe [1] based on the Lambert-Beer's law is used for instantaneous concentration measurement. The light absorptive mateer is the dye called C.I.Direct Blue 86 (Sc ≅ 3,800). The initial concentration of the dye solution C_0 is 3.0kg/m^3. The core diameter of the optical fiber is 10μm, and the gap between the tips of fibers is 0.7mm.

A cold-film sensor (DANTEC 55R11) and the temperature measuring module 90C20 in DANTEC Stream Line are used for instantaneous temperature measurement. In this study, the warm water is issued from the nozzle into the test section. And Prandtl number of the temperature in the water is about 7. The initial temperature difference between the jet water and the ambient water is adjusted to 3K. The length and diameter of the sensing element of cold-film probe are 1.25mm and 70μm, respectively.

The measurement systems by each probe were calibrated before experiments, and the linearity between the output of each measurement system and each physical quantity (velocity, concentration, and temperature) was confirmed.

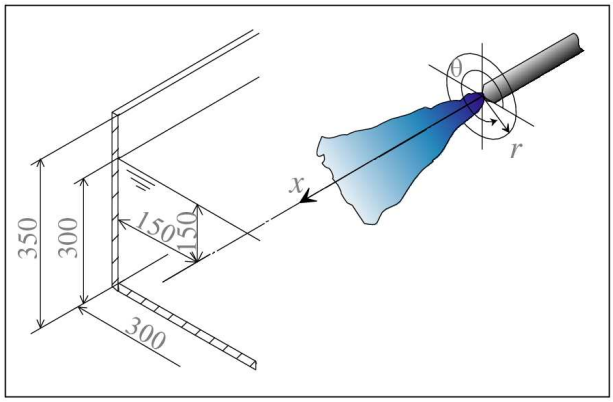

FIGURE 1. SCHEMATIC OF EXPERIMENTAL APPARATUS

RESULT OF VELOCITY MEASUREMENT

Mean Velocity

Figure 2 shows radial profiles of the mean velocity. The horizontal axis is $\langle U \rangle$ normalized by mean velocity on the centerline $\langle U \rangle_c$. The vertical axis is r normalized by b_U. The solid line is the Gaussian curve. From the figure, it is found that radial profiles of x/d=30～50 show a good similarity in each

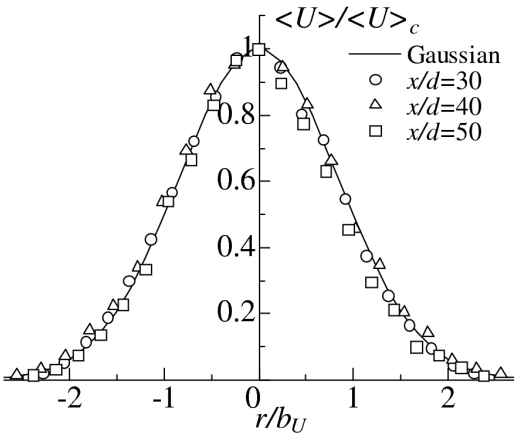

FIGURE 2. RADIAL PROFILES OF MEAN VELOCITY

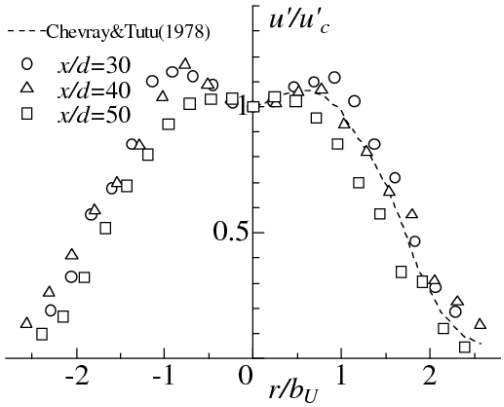

FIGURE 3. RADIAL PROFILES OF THE R.M.S VELOCITY

downstream locations. And their profiles are well approximated by the Gaussian curve.

R.M.S. Values Of Fluctuating Velocity

Figure 3 shows radial profiles of the r.m.s velocity. Horizontal axis is *u'* normalized by r.m.s. values on the centerline u'_c. The vertical axis is *r* normalized by b_U. Radial profiles of the r.m.s velocity have change in the downstream direction. The dashed line in the figure donates the data measured by Chevray & Tutu (1979) [2]. Data of this study show almost the same distribution as the data by Chevray & Tutu (1979) [2].

Probability Density Function (PDF) Of Velocity Fluctuation

Figure 4 shows the downstream variation of the PDF of fluctuating velocity at r/b_U=0. The horizontal axis is *u* normalized by *u'*. The vertical axis is PDF *f(u)* multiplied by *u'*.

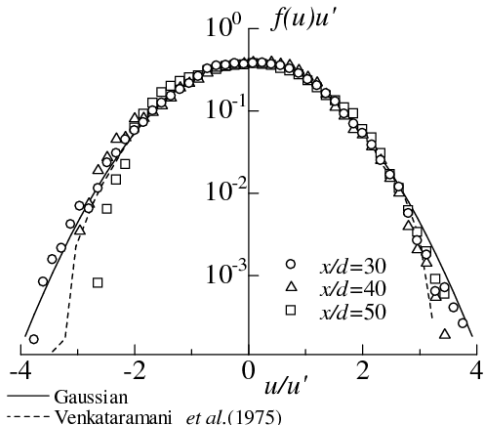

FIGURE 4. DOWNSTREAM VARIATION OF THE PDF OF FLUCTUATING VELOCITY AT r/b_U=0

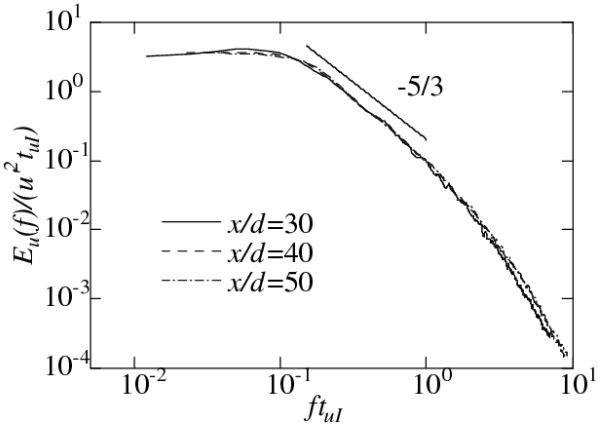

FIGURE 5. POWER SPECTRA OF FLUCTUATING VELOCITY AT r/b_U=0

The solid line is the Gaussian curve. From the figure, it is found that the radial profiles of *x/d*=30～50 show a good similarity in each downstream location. And their profiles are well approximated by the Gaussian curve. The dashed line is the data measured by Venkataramani *et al.*(1975) [3] and it is well in agreement with the distribution of this study.

Power Spectrum Of Velocity Fluctuation

Figure 5 shows the downstream variation of power spectrum of fluctuating velocity on the centerline of the jet (at r/b_U=0). The horizontal axis is the frequency *f* normalized by t_{uI}. The vertical axis is $E_u(f)$ normalized by u'^2 and t_{uI} . This figure displays the spectrum in the frequency range whose maximum corresponds to the length of the sensing element of the hot-film probe (1mm). From this figure, it is found that there exists the range of the -5/3 law.

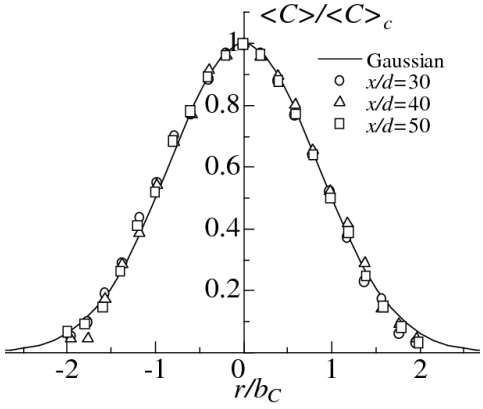

FIGURE 6. RADIAL PROFILES OF MEAN CONCENTRATION

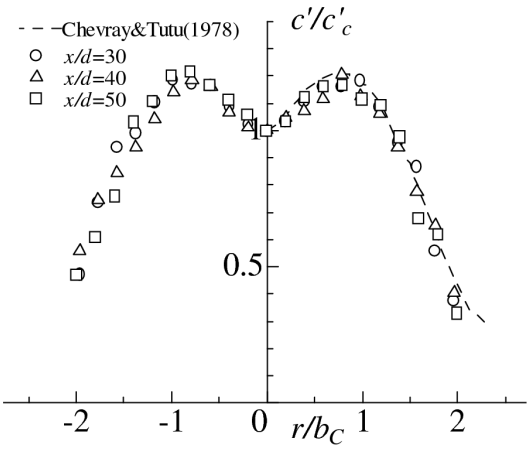

FIGURE 7. RADIAL PROFILES OF THE R.M.S CONCENTRATION

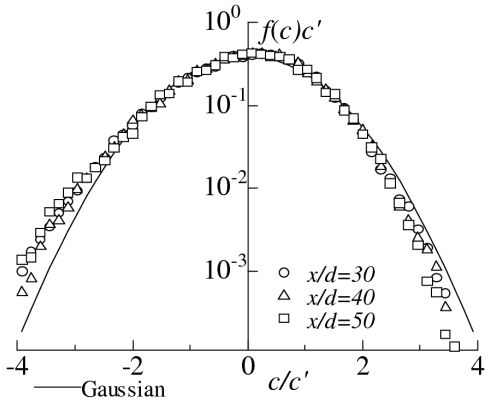

FIGURE 8. DOWNSTREAM VARIATION OF THE PDF OF FLUCTUATING CONCENTRATION AT r/b_c=0

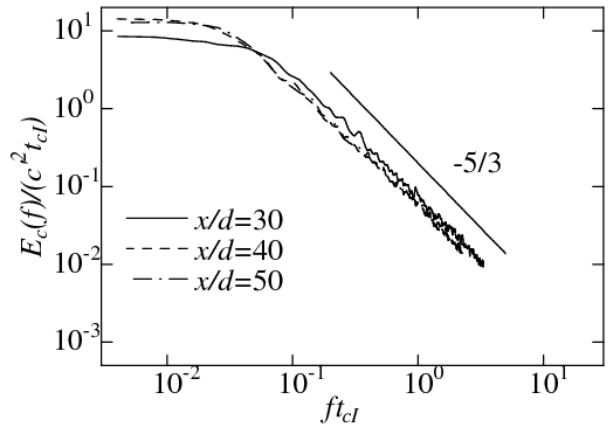

FIGURE 9. POWER SPECTRA OF FLUCTUATING CONCENTRATION AT r/b_c=0

RESULT OF CONCENTRATION MEASUREMENT

Mean Concentration

Figure 6 shows the radial profiles of the mean concentration. The horizontal axis is the $\langle C \rangle$ normalized by mean velocity on the axis $\langle C \rangle_c$. The vertical axis is r normalized by b_C. The solid line shows the Gaussian curve. From the figure, it is found that the radial profiles of x/d=30～50 show a good similarity in each downstream location. And their profiles are well approximated by the Gaussian curve.

R.M.S. Values Of Fluctuating Concentration

Figure 7 shows the radial profiles of the r.m.s. concentration. The horizontal axis is c' normalized by the r.m.s. on the centerline c'_c. The vertical axis is r normalized by b_c. From the figure, the radial profiles of the r.m.s concentration have a similarity of the shape that has a peak value at r/b_C=0.8 in each downstream location. The dashed line in the figure is the data measured by Chevray & Tutu (1979) [2]. Data of this study show almost the same distribution as the data by Chevray & Tutu (1979) [2].

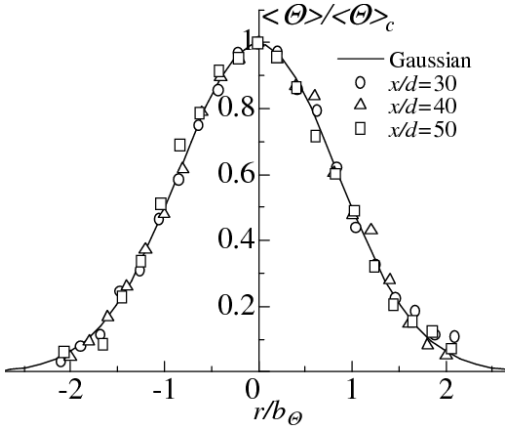

FIGURE 10. RADIAL PROFILES OF THE MEAN TEMPERATURE

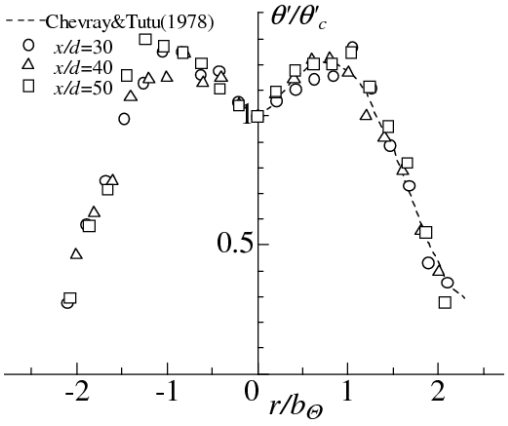

FIGURE 11. RADIAL PROFILES OF THE R.M.S TEMPERATURE

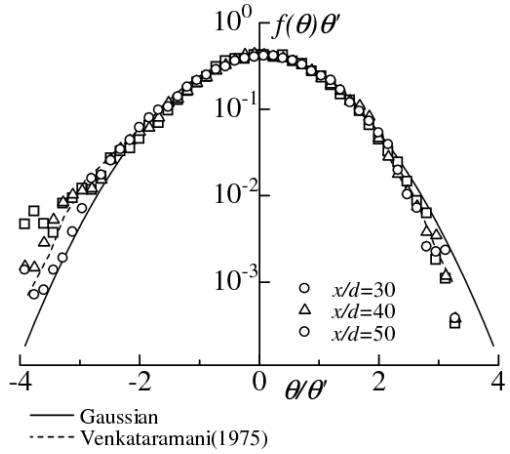

FIGURE 12. DOWNSTREAM VARIATION OF THE PDF OF FLUCTUATING TEMPERATURE AT r/b_Θ=0

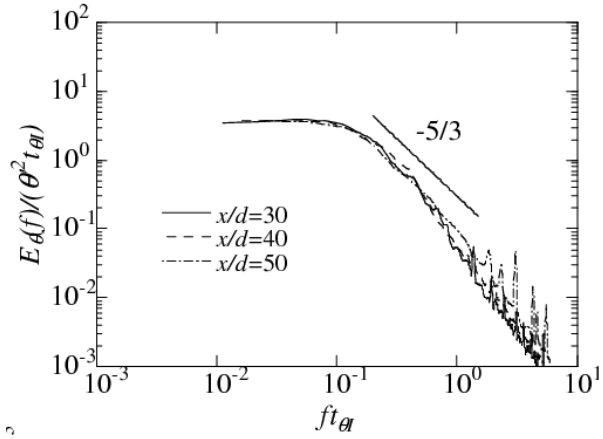

FIGURE 13. POWER SPECTRA OF FLUCTUATING TEMPERATURE AT r/b_Θ=0

Probability Density Function (PDF) Of Concentration Fluctuation

Figure 8 shows downstream variation of the PDF of fluctuating concentration on the centerline of the jet (at r/b_C=0). The horizontal axis is c normalized by c'. The vertical axis is PDF $f(c)$ multiplied by c'. From the figure, it is found that the radial profiles of PDF show a good similarity in each downstream location. It is noted that the PDF of the concentration fluctuation is distorted to negative compared with the Gaussian radial profiles of PDF show a good similarity in each downstream location. It is noted that the PDF of the concentration fluctuation is distorted to negative compared with the Gaussian curve. Here it is worth while referring to the effect of the size of cross-section of the open tank on the PDF profile. Since the size of cross-section of the open tank is about 6.5 times wider than the half width of the concentration at the most downstream position (x/d=50): b_C=22.2mm, the effects of the side wall and free surface seem to be negligible in this experiments.

Power Spectrum Of Concentration Fluctuation

Figure 9 shows the downstream variation of power spectrum of fluctuating concentration on the centerline of the jet (at r/b_C=0). The horizontal axis is the frequency f normalized by t_{cI}. The vertical axis is $E_c(f)$ normalized by c'^2 and t_{cI}. This figure displays the spectrum in the frequency range whose maximum corresponds to the gap between the tips of optical fibers (0.7mm). From this figure, it is found that the range of the -5/3 law spreads gradually as it goes downstream.

RESULTS OF TEMPERATURE MEASUREMENT

Mean Temperature

Figure 10 shows the radial profiles of the mean temperature. The horizontal axis is $\langle \Theta \rangle$ normalized by mean velocity on the axis $\langle \Theta \rangle_c$. The vertical axis is r normalized by b_{Θ}. The solid line in a figure denotes the Gaussian curve. From the figure, it is found that the radial profiles of x/d=30～50 show a good similarity in each downstream location. And their profiles are well approximated by the Gaussian curve.

R.M.S. Values Of Fluctuating Temperature

Figure 11 shows the radial profiles of the r.m.s temperature. The horizontal axis is θ' normalized by the r.m.s. value on the centerline of the jet θ'_c. The vertical axis is r normalized by b_{θ}. From the figure, the radial profiles of the r.m.s temperature show a similarity of the shape with a peak value at r/b_{Θ}=0.8 in each downstream location. The dashed line in the figure denotes the data measured by Chevray & Tutu (1979) [2]. The data of this study show almost the same distribution as the one by Chevray & Tutu (1979) [2].

Probability Density Function (PDF) Of Temperature Fluctuation

Figure 12 shows the downstream variation of the PDF of fluctuating temperature on the centerline of the jet (at r/b_{θ}=0). The horizontal axis is θ normalized by θ'. The vertical axis is PDF $f(\theta)$ multiplied by θ'. The solid line is the Gaussian curve and the dashed line shows the data measured by Venkataramani *et al*. (1975) [3] and it is well in agreement with this study. From the figure, it is found that the radial profiles of PDF show a good similarity, and its similarity profile is distorted to negative side compared with the Gaussian curve like the concentration result (see Fig. 8). Here it is also worth while referring to the effect of the size of cross-section of the open tank on the PDF profile. The size of open tank is about 6.5 times wider than the half width of the temperature at the most downstream position (x/d=50): b_{Θ}=22.9mm, so we can expect that there are almost no effects of the side wall and free surface on the PDF profile.

Power Spectrum Of Temperature Fluctuation

Figure 13 shows the downstream variation of power spectrum of fluctuating temperature on the centerline of the jet (at r/b_{θ}=0). The horizontal axis is the frequency f normalized by t_{uI}. The vertical axis is $E_{\theta}(f)$ normalized by θ'^2 and $t_{\theta I}$. This figure displays the spectrum in the frequency range whose maximum corresponds to the length of the sensing element of the cold-film probe (1.25mm). From this figure, it is found that the range of the -5/3 law spreads gradually as it goes downstream.

COMPARISON OF SPECTRA

Figure 14 shows the comparison of the spectrum for the fluctuating velocity, fluctuating concentration (Sc ≅ 3,800) and fluctuating temperature (Pr ≅ 7) at x/d=50. The horizontal axis is the frequency f normalized by the integral time scale of axial velocity. The vertical axis shows the power spectrum distribution multiplied by some arbitrary constant to make the comparison easier. From the figure, it is found that the temperature spectrum show the -5/3 law in the almost same range as the velocity spectrum, and the concentration spectrum that has high Schmidt number shows the -5/3 law in the wider range than the velocity spectrum. From this, it is found that the shape of spectrum depends on the diffusion coefficient.

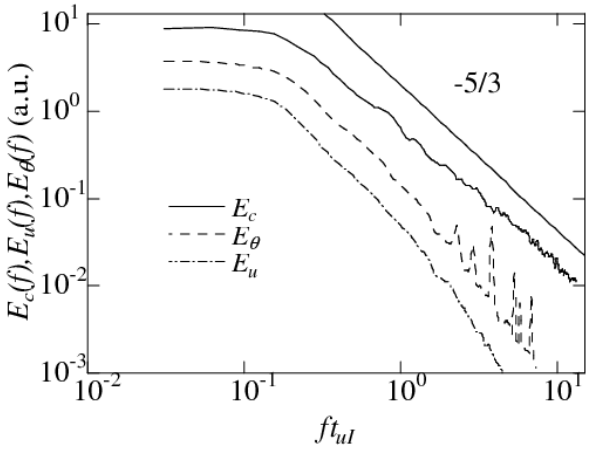

FIGURE 14. COMPARISON OF SPECTRUMS AT x/d=50

DESIGN OF NEW OPTICAL FIBER LIF PROBE

Measurement Principle

When the molecules of fluorescence dye are exited by the laser beam, the energy level of molecules changes from the ground state to the excited state. The excited molecules emit the fluorescence when it is inactivated. This is called the laser-induced fluorescence. In certain condition, the concentration and fluorescence intensity have a linear relationship, so concentration can be obtained from fluorescence intensity by calibrating a proportional constant ahead.

Design Of The Shape Of Optical Fiber Tip

The outline of the new optical fiber probe is explained below. This probe consists of two optical fibers, i.e., one is the fiber for the incidence of laser, and another is the fiber for receiving fluorescence. In addition, the tips of both optical fibers are fabricated into the same spherical shape tips: its tip of which are processed like the shape of a lens. The core diameter of the fiber is 200 μm. Note that the light can not be focused

strictly on one spatial point because of the difference of refraction angle passing thorough the spherical surface of the fiber tips, so in this design, the width of the laser beam is defined as a sampling volume (which is called focal width). We aimed that the width of the laser beam is under several micrometers and the length from the tip to the measurement point which is called focal length is several millimeters. The focal length ant the focal width calculated in this study is shown Tab. 1.

TABLE 1. MEASUREMENT OF OPTICALFIBER TIP

Type	r (μm)	Focal Length (μm)	Focal width (μm)
A	500	5590	1.2
B	600	6750	0.8
C	650	7320	0.6

From Tab. 1 it is found that the laser beam is enough narrower than the optical fiber sensor (core diameter is 10 μm) which is used for the concentration measurement in this study. Here type C is adopted as the shape of the fiber tip. As presented in Tab. 1 the length to the measurement point (focal length) is about 7.3 mm, the width of the beam at measurement point is about 0.6 μm. Now it is evaluated whether this width is sufficient size to measure the Batchelor scale. In this study Fluorescein sodium (Sc=1,900) is used for LIF measurement. Figure 15 shows the downstream variation of each scale on the jet axis in the concentration measurement condition in this study (Re_D=20,000, d=4mm). The horizontal axis is x normalized by d. The vertical axis is each scale normalized by d. The dashed line is the Taylor scale, the chain line is the Kolmogorov scale and chain double dashed line is Batchelor scale. Also, l_A is the length of the cold-film sensor used temperature measurements, l_B is the gaps between two tips of optical fibers and l_C is the focal width of optical fiber LIF probe designed in this study. The Taylor scale λ and the Kolmogorov scale η on the jet axis are estimated by Eq. (1), (2) that are proposed by Friehe *et al* (1972)[4].

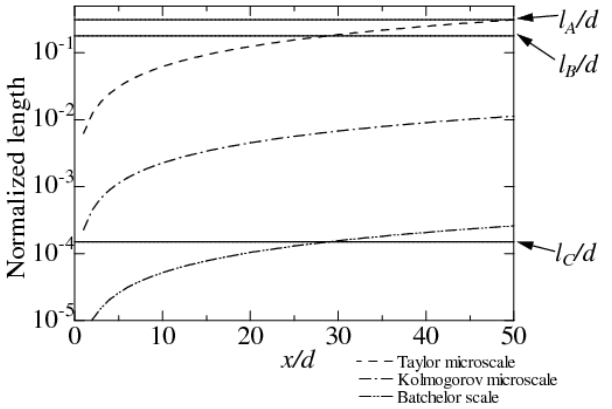

FIGURE 15. EXAM OF FOCAL WIDTH

$$\frac{\lambda}{d} = 0.88\,\mathbf{Re}^{-1/2}\,\frac{x}{d} \tag{1}$$

$$\frac{\eta}{d} = \left(43\,\mathbf{Re}^{3}\right)^{-1/4}\,\frac{x}{d} \tag{2}$$

And the Batchelor scale η_θ is calculated by Eq. (3).

$$\eta_\theta = \frac{\eta}{Sc} \tag{3}$$

From the Fig. 15, it is found that the LIF probe of type C has the resolution less than η_θ at $x/d \geq 30$. So experiments using this LIF probe will be conducted in the downstream region of $x/d \geq 30$.

DESIGN OF THE EXPERIMENTAL SET UP

Figure 16 shows schematic of experimental set up and Fig. 17 shows configuration of fiber probes and measuring point. The laser beam is transmitted to the neighborhood of the measurement point by the fiber for the incidence. This makes minimizes the influence of attenuation of the laser light. In addition, narrow focal width enables us to measure the concentration in much smaller sampling volume than before. Two optical fibers are arranged so that the focuses of both fibers may overlap to receive fluorescence at only measurement point efficiently. Because the focal width is order of sub-micrometer, position setting of fibers is performed using highly precise adjustment equipment. The received fluorescence is transmitted to the Photomultiplier Tube (PMT) by another fiber for receiving fluorescence. The data are stored to the PC.

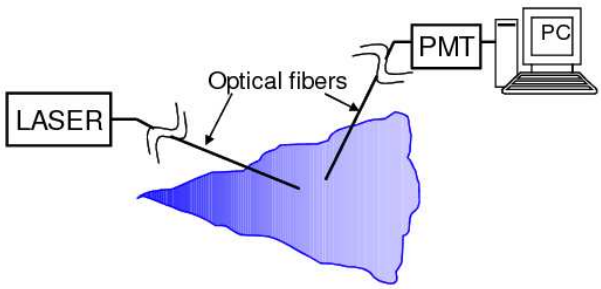

FIGURE 16. SCHEMATIC OF EXPERIMENTAL SET UP

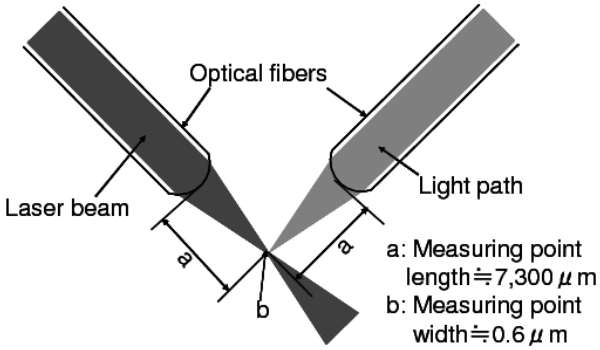

FIGURE 17. SCHEMATIC OF FIBER PROBES AND MEASUREING POINT

CONCLUSION

In this study, in an axisymmetric turbulent jet, the velocity, the concentration and the temperature are measured by the hot-film probe, the fiber probe and the cold-firm probe, respectively. The conclusions are as follows. It is found that the concentration spectrum has wider range of the -5/3 law than temperature spectrum. This result means that the shape of spectrum depends on the diffusion coefficient.

In order to obtain the higher resolution for the measurement of concentration, a new optical probe based on the LIF method is designed. The tip shape of optical fiber LIF probe is newly designed. In the present design, the width of focus of laser beam is set to 0.6 micrometers. It is shown that this probe has the resolution less than the Batchelor scale at $x/d \geq 30$ on the jet axis in the condition of the present jet diffusion field of a high Schmidt number matter (d=4mm, Re=20,000).

REFERENCES

[1] Y. Sakai *et al*., 2006. "Velocity-Scalar Joint Statistics in the Jet Diffusion Field of High Schmidt-Number Matter". *Transactions of the Japan Society of Mechanical Engineers. B.* Vol. 72(732). pp. 2702-2709.

[2] R. Chevray and N.K. Tutu, 1979 "Intermittency and preferential transport of heat in a round jet". *J. Fluid Mech*. Vol. 88. pp. 133-160.

[3] K.S. Venkataramani, 1975 "Probability distributions in a round heated jet" *Phys. Fluids*. Vol. 18. pp. 1413-1420.

[4] C.A. Friehe, C.W. Van Atta, and C.H. Gibson, "Jet turbulence: dissipation rate measurements and correlation" *Turbulent Shear Flow*. No. 93. pp18.1-18.7.